Euro. Jnl of Applied Mathematics (2017), *vol.* 28, *pp.* 357–379.
doi:10.1017/S0956792516000310

Unsteady flows induced by a point source or sink in a fluid of finite depth

T. E. STOKES[1], G. C. HOCKING[2] and L. K. FORBES[3]

[1]*Department of Mathematics, University of Waikato, Hamilton, New Zealand*
email: *stokes@waikato.ac.nz*
[2]*Mathematics and Statistics, Murdoch University, Murdoch, Western Australia, 6150, Australia*
email: *G.Hocking@murdoch.edu.au*
[3]*School of Mathematics and Physics, University of Tasmania, GPO Box 252-37, Hobart 7001, Australia*
email: *Larry.Forbes@utas.edu.au*

(*Received 25 November 2014; revised 15 June 2016; accepted 15 June 2016; first published online 22 July 2016*)

The time-varying flow in which fluid is withdrawn from or added to a reservoir of infinite or arbitrary finite depth through a point sink or source of variable strength beneath a free surface is considered. Backed up by some analytic work, a numerical method is used, and the results are compared with previous work on steady and unsteady flows. In the case of withdrawal for an impulsively started flow, it is found that the critical flow rate increases with reservoir depth, although it changes little as the depth increases beyond double the sink submergence depth. The largest flow rate at which steady solutions can evolve in source flows follows a similar pattern although at a considerably higher value. Simulations indicate that some of the previously calculated steady state solutions at higher flow rates may be unstable, if they exist at all.

Key words: Free-surface potential flows, ideal fluids

1 Introduction

Withdrawal of water from reservoirs for drinking and irrigation is a problem of particular importance in dry climates or where fresh water is limited by saline intrusions or other pollutants. Beginning as early as 1901 a series of papers such as [1, 7, 16–18, 20, 21, 24, 34] addressed this issue by considering steady flows into outlets of various dimensions from fluids with a range of stratification patterns. In most cases, the authors were seeking the critical parameters at which the withdrawn fluid begins to include potentially undesirable water, e.g. salty or polluted, from different layers. Later, steady solutions computed numerically [2–6, 8, 10–13, 30, 31] found very accurate values for the limiting steady state solutions, but were not always clear in determining the critical transition to two layer flows, as in some cases, there appeared to be gaps between maximal steady flows and cusped critical flows. In addition, experimental results [9] did not always agree well with computations. Xue and Yue and others [19, 23, 33] computed unsteady solutions numerically, but again had difficulty in computing solutions beyond a certain time and hence in finding critical transition values.

More recently, Stokes *et al.* [26, 28] performed a detailed analysis of unsteady flow into a line sink in water of infinite depth and finite depth, respectively, and compared their

results with the existing steady solutions. They found that there are at least two critical values of the flow rate parameter at which drawdown (the transition to two layer flow) can occur, depending on the flow history. For example, an impulsively started flow may drawdown immediately and at a lower flow rate than if the flow is gradually increased. In the infinite depth case, they showed that steady flows exist up to some critical value. However, for finite depth, two-dimensional flows, such steady flows cannot strictly arise. As observed in [19] and [28], there is a local shift in fluid depth (starting above the sink) which propagates outward across the fluid domain at a fixed velocity. This adjustment is well predicted by shallow water theory, but applies to some extent to fluids of any finite depth. For this reason, the fluid never approaches a steady flow except near to the region of the submerged sink, where the characteristic shape of a stagnation point steady flow is discernible: see [19] and [28]. There are thus significant differences in the flow pattern induced in fluids of finite and infinite depth.

These ideas were extended in [15, 27] to consider the case of a point sink in a fluid of infinite depth. Again, the results showed that the critical drawdown parameters depended on the history of the flow, and that past steady and experimental work needs to be examined in this light. In general, the behaviour was found to be qualitatively very similar to the infinite depth line sink case [26]. In [15], Hocking *et al.* showed that a simple rational approximation could be obtained based on the solution to the linearised equations and that this performed well in comparison with the full non-linear solution at small values of the flow rate and if the variation in the flow rate was small. The question arises, given the differences between finite and infinite depth in the two-dimensional flow, whether a similar difference exists in the case of a point sink in axisymmetric flow. In principle, there is less difference between them because as one moves away from the outlet, the fluid speed must approach zero in both cases, unlike the two-dimensional case in which the fluid in finite depth can approach a constant, non-zero speed.

Here, we consider this issue in addition to attempting to quantify the critical parameters for a range of flow geometries for a point sink in a fluid of finite depth.

2 Problem formulation

The axisymmetric, unsteady, irrotational flow of an inviscid, incompressible, fluid of finite depth into a point sink beneath a free surface is considered. The assumption of radial symmetry means the problem can be reduced to finding the free surface profile as a function of radial distance from the origin.

Consider a point sink at depth h beneath the undisturbed level of the free surface, $\hat{z} = 0$, which has strength $m = m(\hat{t})$, where $\hat{t}$ is time. The channel has depth $\hat{H}$.

We can define a velocity potential $\hat{\phi}(\hat{r}, \hat{z})$ such that $\hat{\mathbf{v}} = \nabla\hat{\phi}$ is the velocity vector for the flow and satisfies

$$\nabla^2\hat{\phi} = 0, \quad \hat{z} < \hat{\eta}(\hat{r}, \hat{t})$$

throughout the fluid domain except at the point $(\hat{r}, \hat{z}) = (0, -h)$, the location of the singularity representing the point sink, and where $\hat{z} = \hat{\eta}(\hat{r}, \hat{t})$ is the equation of the free

https://doi.org/10.1017/S0956792516000310 Published online by Cambridge University Press

surface. As this point is approached, the velocity potential satisfies

$$\hat{\phi} \to \frac{m}{4\pi} \frac{1}{\sqrt{(\hat{r})^2 + (\hat{z}+h)^2}} \quad \text{as} \quad (\hat{r}, \hat{z}) \to (0, -h).$$

The requirement that there be a solid, horizontal boundary at depth $\hat{z} = -\hat{H}$ forces $\hat{\phi}_z = 0$ on $\hat{z} = -\hat{H}$, which can in many cases be satisfied by demanding that an image sink be placed symmetrically below the base of the channel.

The conditions on the free surface are the dynamic condition of atmospheric pressure on the free surface, which comes from the Bernoulli equation, i.e.

$$\hat{\phi}_{\hat{t}} + \frac{1}{2}(\hat{u}^2 + \hat{v}^2) + g\hat{\eta} = 0 \quad \text{on} \quad \hat{z} = \hat{\eta}(\hat{r}, \hat{t}), \tag{2.1}$$

and the kinematic condition

$$\hat{\eta}_{\hat{t}} + \hat{\phi}_{\hat{r}}\hat{\eta}_{\hat{r}} - \hat{\phi}_{\hat{z}} = 0 \quad \text{on} \quad \hat{z} = \hat{\eta}(\hat{r}, \hat{t}), \tag{2.2}$$

stating that the fluid may not cross its own boundary.

To allow the sink strength m to be viewed as a function of time, we do not include it in our non-dimensionalisation; this is the approach taken in [15] and [28]. As in [15], which concerned linearised solutions to the axisymmetric infinite depth withdrawal problem in which the sink strength was a function of time, we non-dimensionalise using the length scale h, the time scale $\sqrt{h/g}$, and hence a velocity scale of $\sqrt{gh}$, and a velocity potential scale of $h\sqrt{gh}$.

The dimensionless equations are then

$$\nabla^2\phi = 0, \quad z < \eta(r,t), \quad \mathbf{r} \neq (0,-1), \tag{2.3}$$

where $\mathbf{v} = \nabla\phi$ subject to

$$\phi_t + \frac{1}{2}(u^2 + v^2) + \eta = 0 \quad \text{on} \quad z = \eta(r,t), \tag{2.4}$$

and

$$\eta_t + \phi_r\eta_r - \phi_z = 0 \quad \text{on} \quad y = \eta(r,t), \tag{2.5}$$

with the extra conditions that

$$\phi \to \frac{F}{\sqrt{r^2 + (z+1)^2}} \quad \text{as} \quad (r,z) \to (0,-1) \tag{2.6}$$

near the sink, and

$$\phi_z = 0 \quad \text{on } z = -H \tag{2.7}$$

at the bottom of the fluid.

Here, H is the dimensionless depth of the fluid and the *Froude number* is defined to be the function of time

$$F(t) = \frac{m(t)}{4\pi\sqrt{gh^5}}.$$

https://doi.org/10.1017/S0956792516000310 Published online by Cambridge University Press

The most important quantities are the Froude number $F(t)$, whose variation over time is caused only by variation in m, and the fluid depth H. In addition, there must be initial conditions on the problem and the most common is that the flow is initiated from a quiescent situation at time $t = 0$, so that

$$\phi(r, z, 0) = 0 \text{ on } z = \eta(r, 0) = 0. \tag{2.8}$$

3 Asymptotics

Much information can be gleaned from finding asymptotic solutions for small or slowly varying Froude number. For example, the change in local depth in the two-dimensional finite depth case [28] is well described by a first-order linearised solution. Likewise, in the infinite depth point sink problem [15], a Froude number expansion provided an excellent representation of the development of the free surface as the flow rate was increased and a rational approximation was obtained that performed very well in simulating a variety of subcritical flows. It is therefore worthwhile to consider such solutions here, both for the insight provided and also to verify the numerical scheme.

3.1 The linearised problem

In the finite-depth situation, the linearised problem is to find a solution to Laplace's equation for the velocity potential, subject to a sink present at $(r, z) = (0, -1)$, that is,

$$\phi \to \frac{F(t)}{\left[r^2 + (z+1)^2\right]^{1/2}} \quad \text{as } (r, z) \to (0, -1),$$

where $F(t) = F_0 f(t)$ is the time-dependent sink/source intensity. If we assume F_0 to be small and $f(t)$ to be of order 1, then we can linearise in terms of F_0 and the conditions on the free surface become

$$\begin{aligned} &\eta_t = \phi_z \text{ and } \phi_t = -\eta \text{ on } z = 0 \\ &\quad \Rightarrow \phi_{tt} + \phi_z = 0 \quad \text{on } z = 0, \end{aligned} \tag{3.1}$$

with condition (2.7) being satisfied at the bottom $z = -H$. This problem is considered in [32]; see Section 10 where expansion in a small parameter is considered. We observe that a linearised solution of this type is only available in this unsteady flow, since at this order of approximation, the steady free-surface conditions (3.1) would reduce simply to a flat interface on the plane $z = 0$. Such an approach to linearisation is only possible in unsteady flow and leads to our conditions (3.1).

In the steady case, linearisation is not available, and instead, asymptotic techniques are needed; these show that the steady interface is proportional to F_0^2. One such approach is outlined briefly in Section 3.2. For the case of a line source, such asymptotic approaches are well-known; recently, a higher order method is given by Lustri *et al.* in [22].

https://doi.org/10.1017/S0956792516000310 Published online by Cambridge University Press

We choose a form that satisfies all of these conditions except (3.1), that is

$$\phi(r,z,t) = \frac{F(t)}{\left[r^2+(z+1)^2\right]^{1/2}} + \frac{F(t)}{\left[r^2+(z-1+2H)^2\right]^{1/2}} + \int_0^\infty A(k,t)J_0(kr)\cosh k(z+H)\,dk. \tag{3.2}$$

The first two terms satisfy the bottom condition (2.7), whilst the integral also satisfies this by the choice of the cosh term. All terms satisfy Laplace's equation (2.3), except at the sink itself.

Although it is possible to work in greater generality, the analysis is more straightforward if we restrict attention to a particular form for $F(t)$. The one we consider is an exponential that asymptotically approaches a final value, a case we use frequently in the numerical simulations and which can also be used to model other flows by taking suitable limits. Thus, we assume $F(t) = F_0(1-e^{-\alpha t})$ for some $\alpha > 0$. Here, $F(0) = 0$, and $F(t) \to F_0$ as $t \to \infty$. For large α, the flow approximates the impulsive flow $F = F_0$ after a short transient phase, whilst for small α, it approximates a linearly increased flow $F \approx F_0\alpha t$ for small to moderate t. (By contrast, the case of a submerged source/sink considered in [32] is that in which $F(t) = F_0\cos(\sigma t)$.)

With this choice of $F(t)$, substituting (3.2) into (3.1), we obtain the general solution for $A(k,t)$ as

$$A(k,t) = C_1(k)\cos\lambda t + C_2(k)\sin\lambda t + F_0\left(\frac{G(k)}{\sinh kH} + \frac{(\alpha^2-k)G(k)e^{-\alpha t}}{\alpha^2\cosh kH + k\sinh kH}\right), \tag{3.3}$$

where $\lambda = \sqrt{k\tanh kH}$, and $G(k) = e^{-k} + e^{-(2H-1)k}$. The initial conditions must be used to determine $C_1(k)$ and $C_2(k)$; these are

$$\phi(r,0,0) = 0 \quad \text{and} \quad \eta(r,0) = 0 \quad \text{on } z = 0. \tag{3.4}$$

After some further work, these conditions reveal that

$$C_1(k) = \frac{-2\alpha^2F_0\cosh(k(H-1))}{\sinh kH(\alpha^2\cosh kH + k\sinh kH)}, \tag{3.5}$$

$$C_2(k) = -\frac{-2\alpha kF_0\cosh(k(H-1))}{\lambda\cosh kH(\alpha^2\cosh kH + k\sinh kH)}. \tag{3.6}$$

Substituting (3.5) and (3.6) into (3.3), then (3.3) into (3.2), invoking (3.1) on $z = 0$, and replacing the sink terms by integrals, we obtain the integral form

$$\eta(r,t) = -2\alpha F_0\int_0^\infty \frac{J_0(kr)\cosh k(H-1)}{(\alpha^2\cosh kH + k\sinh kH)} \times \left(ke^{-\alpha t} + \alpha\lambda\coth(kH)\sin(\lambda t) - k\cos(\lambda t)\right)\,dk. \tag{3.7}$$

This can be evaluated to high precision using a numerical quadrature routine such as those provided in the package MATLAB.

https://doi.org/10.1017/S0956792516000310 Published online by Cambridge University Press

Two further cases of interest for $F(t)$ can be obtained from this one, for subsequent comparison with the numerics. The impulsive case, in which $F = F_0$ for all t, can be viewed as the limit of the exponential ramp-up case in which $\alpha \to \infty$, so that the exponential term decays away extremely rapidly. Similarly, the case of a linear ramp-up from zero may be viewed as a limiting case in which $\alpha \to 0$ and $F_0 \to \infty$ in such a way that αF_0 is non-zero and finite: For small to moderate t, the resulting solution will then behave like the linear ramp-up case $F(t) = \alpha F_0 t$. These two analytic limits will not coincide precisely with the formal solutions obtained by linearising using the corresponding choices of $F(t)$: In particular, the $\alpha \to 0$ case will not resemble the ramped-up case for sufficiently large t, since $f(t)$ in $F(t) = F_0 f(t)$ will not remain order 1. However, they provide useful benchmarks for comparison with the numerics, and in practice agreed well with the results of numerical experiments if flow rates were low to moderate (with a partial exception in the impulsive case, to be discussed shortly).

3.2 An approximate solution

In [15], a two-term rational approximation to $\eta(t)$ in response to a small, slowly varying flow rate $F(t)$ was obtained in the case of a source or sink submerged in a fluid of infinite depth. This was justified theoretically for cases where $F(t)$ was a linear function, and shown to apply in a wide variety of more general cases (at least following a short transient period). The flow was a perturbation to a steady flow, in which the surface profile $\eta(t)$ consisted of a dip term proportional to $F'(t)$, and a stagnation point term, proportional to $F(t)^2$. The latter term was the asymptotic stagnation point steady flow (in which the central point sits at the stagnation point level of $z = 0$) that would evolve at the appropriate value of F. The dip term was found to remain stable for a considerable time in the case of a linear increase in flow rate once the transient terms had passed.

The superposition of these two terms proved to be an extremely good predictor of the flows generated numerically using the full non-linear equations for a surprisingly wide range of possible flow functions $F(t)$ – see [15]. Indeed the same thing is observed in the current finite depth setting, although the rigorous analytic justification of this (even for linear $F(t)$) is very complex. (Examples of this dip term are given for various choices of H in Figure 6.)

Instead, we give a heuristic argument similar to that given initially in [15]. Assume that the flow potential is given approximately using a separation of variables type approach by $\phi(r, z, t) = F(t)\phi^{(s)}(r, z)$. Using equation (2.4), we obtain on $z = 0$,

$$\begin{aligned}\eta &= -\phi_t - \frac{1}{2}(u^2 + v^2)\\ &\approx -F'(t)\phi^{(s)}(r,0) - \frac{1}{2}F(t)^2\phi_r^{(s)}(r,0)^2\\ &= -F'(t)y_1(r) - F(t)^2 y_2(r),\end{aligned} \tag{3.8}$$

where

$$y_1(r) = \phi^{(s)}(r,0) \quad \text{and} \quad y_2(r) = \frac{1}{2}\phi_r^{(s)}(r,0)^2. \tag{3.9}$$

https://doi.org/10.1017/S0956792516000310 Published online by Cambridge University Press

Note that an asymptotic stagnation point steady solution may be obtained by assuming $F(t)$ is a small constant; then, the first term drops out and one is left with an order F^2 asymptotic steady solution. In contrast to the infinite depth case covered in [15], neither y_1 nor y_2 has a simple closed form, although it is clear from the simulations that the term $-F'(t)y_1(r)$ is a dip (or bulge if $F'(t) < 0$) centred on $r = 0$ and proportional in size to the rate of change of $F(t)$, whilst the term $-F(t)^2 y_2(r)$ is the stagnation point steady state surface that would evolve at the current value of F. In the infinite depth case, these two terms are combined as in (3.8) to provide a simple simulation of a linearly increased flow in which transient waves are ignored; comparison with the full simulations was surprisingly good, even for non-linear slowly varying sub-critical flow functions $F(t)$. Note that the dip term $-F'(t)y_1(r)$ is a solution to the linearised equations, although not one satisfying the initial condition that $\eta(r, 0) = 0$ for all r.

Of course, this argument is not rigorous, but it is clear in the simulations that both the dip term and the stagnation point steady state term play a significant role in the behaviour of the free surface, for a wide range of possible choices of $F(t)$ (but especially when it is linear), and they provide convenient terms of reference for the discussion of results that follows.

4 The numerical method

A numerical method based on that employed in [27] for the three-dimensional axisymmetric point sink case is considered. These schemes are very similar to those described in Scullen and Tuck [25], and Tuck [29]. It is a semi-Lagrangian approach in which we follow the evolution of concentric rings centred above the sink on the free surface subject to an evolving potential. Radial symmetry guarantees that all points on such a ring have the same elevation. The surface is discretised into N rings and a recursive process is used to update the global velocity potential and the heights of the N rings on the free surface at each time step. We can specify the position of one such ring by giving its radius and height, thereby reducing the description of the free surface to two parameters. A detailed description is given in these earlier works and so what follows is a summary of the main features of the method.

4.1 Equation formulation

Initially, we assume the sample rings are at rest and in some fixed positions $(R_i^{(0)}, Z_i^{(0)}), i = 1, \ldots, N$ on the free surface, for which we always assume $Z_i^{(0)} = 0, i = 1, \ldots, N$. We track the velocity potential function at points on the free surface. To reflect the initial condition of quiescence, we assume it is zero everywhere on the free surface initially: $\Phi_i^{(0)} = 0, i = 1, \ldots, N$ is the flux at time $t = 0$ at the ith point on the surface.

The recursive step modifies each ring's position and the coefficient of the associated potential function everywhere in the fluid by solving a Dirichlet problem. Thus, if at time step t, the ith ring has coordinates $(R_i^{(t)}, Z_i^{(t)})$ and the global velocity potential is $\phi^{(t)}(r, z)$ at all points (r, z) in the fluid, so that $\Phi_i^{(t)} = \phi(R_i^{(t)}, Z_i^{(t)}), i = 1, \ldots, N$ is the velocity potential function on the surface, then the time evolution of all points is given by (dropping the

https://doi.org/10.1017/S0956792516000310 Published online by Cambridge University Press

time superscript for simplicity):

$$\frac{dR_i}{dt} = u_i \tag{4.1}$$

$$\frac{dZ_i}{dt} = v_i \tag{4.2}$$

$$\frac{d\Phi_i}{dt} = \frac{1}{2}\left[(u_i)^2 + (v_i)^2\right] - Z_i. \tag{4.3}$$

Here, $u_i = \phi_r(R_i, Z_i)$ and $v_i = \phi_z(R_i, Z_i)$, where the derivatives are with respect to r following the free surface. (We used finite differences to perform these slope calculations.) Hence, the values of R_i, Z_i and Φ_i can be evolved forward one time step. The task remains to determine $\phi^{(t+1)}$ from these $\Phi_i^{(t+1)}$.

Assume radii and elevations $P_i = (R_i, Z_i), i = 1, \ldots, N$ for the free surface rings at time step t, and values $\Phi_i, i = 1, \ldots, N$ for ϕ given at each. Choose the ring sink with radius and elevation $(\rho_i, \zeta_i), i = 1, \ldots, N$ outside the fluid domain and normal to the free surface ring given by (R_i, Z_i). The presence of the base forces requires that $\phi_z = 0$ on $z = -H$, a condition that is satisfied by the introduction of an image ring sink for each such ring sink, having the same radius but positioned as far below the base as the original was above, namely at $Z = -Z_i - 2H$.

The potential at a given point (r, z), due to the submerged sink one unit below the origin (together with its needed image sink below the base) is

$$\Phi_s(r, z) = F(t)\left(r^2 + (z+1)^2\right)^{-1/2} + F(t)\left(r^2 + (z-1+2H)^2\right)^{-1/2}.$$

Additionally, for the ith ring sink, the contribution to the total potential at the point $(x, y, z) = (r\cos\alpha, r\sin\alpha, z)$ will be a multiple of $\Phi_i(r, z) = \Phi_{1,i}(r, z) + \Phi_{2,i}(r, z)$, where

$$\Phi_{1,i}(r, z) = \int_0^{2\pi} \frac{\rho_i}{\left[r^2 + \rho_i^2 + (z - \zeta_i)^2 - 2r\rho_i\cos(\theta - \alpha)\right]^{1/2}} d\theta$$

and

$$\Phi_{2,i}(r, z) = \int_0^{2\pi} \frac{\rho_i}{\left[r^2 + \rho_i^2 + (z + 2H + \zeta_i)^2 - 2r\rho_i\cos(\theta - \alpha)\right]^{1/2}} d\theta,$$

by a strength factor to be determined.

Each such sum of two integrals can be expressed as a linear combination of elliptic integrals of the first and second kinds, and evaluated using standard series expansions. Thus, we assume a series that satisfies Laplace's equation everywhere within the fluid, of the form

$$\phi(r, z) = \Phi_s + \sum_{i=1}^{N} q_i \Phi_i.$$

https://doi.org/10.1017/S0956792516000310 Published online by Cambridge University Press

The source strengths $q_i, i = 1, \ldots, N$ are unknown constants that are determined once the values of ϕ are given at N distinct points, from which we obtain N linear equations in the q_i and solve to give $\phi(r, z)$.

Differentiating under the integral signs in the previously obtained expression for ϕ allows us to compute $u = \phi_r$ and $v = \phi_z$, which again can be readily computed in terms of elliptic integrals. This allows us to compute the fluid velocities $(u_i, v_i), i = 1, \ldots, N$ at time $t + 1$.

4.2 Computational details

Following Scullen and Tuck [25], and Tuck [29], initially, discrete points along the free surface were distributed with even spacing near $r = 0$ and a geometric increase in spacing beyond a certain point, so that for i sufficiently large, $\delta r_i = \gamma \delta r_{i-1}$, where γ is some constant slightly greater than 1, with δ_i constant for smaller i. However, it was found that for runs with many points and a small spatial increment, the point of transition from even spacing to wider and wider spacing would lead to numerical instabilities (especially with sink flows), and it became necessary to ensure that the horizontal spatial increment changed smoothly. One solution to this was to allow the expansion of the spatial increment to begin from $i = 0$.

For long runs in which steady states were sought, there were two main requirements: high accuracy near $r = 0$, where the surface deflection was greatest, and a very wide computational domain to avoid spurious numerical reflections. To fulfil these requirements without the use of an unfeasibly large number of domain points, it was found that a spatial increment that increased at a uniform rate from $r = 0$ was not satisfactory: either accuracy would be too low around $r = 1$, or the computational domain would be too narrow. Instead, the rate of increase was made small near $r = 0$, and then became larger away from $r = 0$, but varied smoothly across the domain to avoid the instabilities described above. We used the following formula:

$$\delta r_i = (1 + (\gamma - 1)(1 + i/200))\delta r_{i-1}.$$

The initial value of δr was chosen to be 0.005, with $\gamma = 1.005$, meaning a very slight attenuation of domain points near $r = 0$, with the degree of stretching doubling by $i = 200$. On the longest runs, 600 points were used, meaning a very small spatial increment of 0.005 very close to $r = 0$, around 0.012 near $r = 1$ and still only around 0.021 near $r = 2$, yet also a computational domain going out to $r \approx 473$. This proved sufficient to give stable, converged solutions for runs lasting as long as $t = 200$, a far higher degree of accuracy than that used in either [33] or [27].

The sink locations were chosen as in [26]. It was found that including a point sink above the surface at $r = 0$ caused numerical instabilities, and so the smallest radius ring sink was placed at $r = \delta r/2$, where δr was the local surface point separation distance close to $r = 0$. It was found that reliable simulations could be obtained if the distance of the ring sinks above the free surface was chosen to be three times the local grid spacing, i.e. $3\delta r$; this choice is consistent with earlier work, and has been found to give consistent solutions by trial and error. Splines were used to re-position points along the free surface

https://doi.org/10.1017/S0956792516000310 Published online by Cambridge University Press

according to the original R-spacings, using an arclength type calculation as described in [26].

For long runs in which steady states were sought (running to $t = 200$), a relatively large time increment of $\delta t = 0.025$ was used. But for short runs involving impulsively initiated flows and very rapid changes in surface profile (running for $t \approx 1$ or less), a much smaller time increment was needed to give sufficient accuracy: typically $\delta t = 0.002$ was used for impulsive constant strength flows, with even smaller values for the other cases. Experimentation revealed when a sufficiently small value of δt was being used (so that making the value even smaller made a negligible difference to results).

We used *Fortran* to perform the simulations and then viewed the results using *Matlab*. The result was a series of "movies" of the evolution of the free surface in cross-section.

5 Results of numerical experiments

The approach in this work is very similar to that of earlier papers in this series. Again, it turns out that there are different critical flows for different histories. In what follows we compare the full simulations with the linear and approximate solutions described above and then go on to determine the critical flow parameters.

5.1 Comparison with the linear solution: sub-critical flows

For large fluid depth H, the simulations at small flow rates, with constant, linearly increased, and exponentially increased flow rate functions $F(t)$, respectively, were closely matched by the corresponding linearised solutions in all cases, in much the same manner as in [15]. However, as the depth of the layer approached the sink from below, i.e. as H approached unity, the linearised solution seemed to depart from the output of the simulations as t increased.

This resulting discrepancy is shown in Figure 1 for the worst case $H = 1$ at four different times, with sink strength having constant Froude number $F = 10^{-3}$: The two surfaces have the same basic shape but there is a clear difference in elevation which peaks around $t = 4$ (at least at $r = 0$). Roughly, the same difference in elevation occurred regardless of what shape function for $F(t)$ was used, and seemed to be roughly of order F for small F. The two solutions are in very close agreement during the initial drawdown phase, but they drift away from each other subsequently in the early stages of the long slow return-to-zero phase. However, this observed gap is not inconsistent with properties of linearisations, since the linearised solution can return to zero at a different rate to the full non-linear solution.

Overall then, these comparisons provide confidence in the numerical results and also provide some solid insight into the flow evolution.

5.2 Impulsively initiated constant strength flows

We next consider the classic problem of an impulsively initiated flow, in which the Froude number shifts discontinuously from 0 to some fixed value at time $t = 0$, remaining constant thereafter.

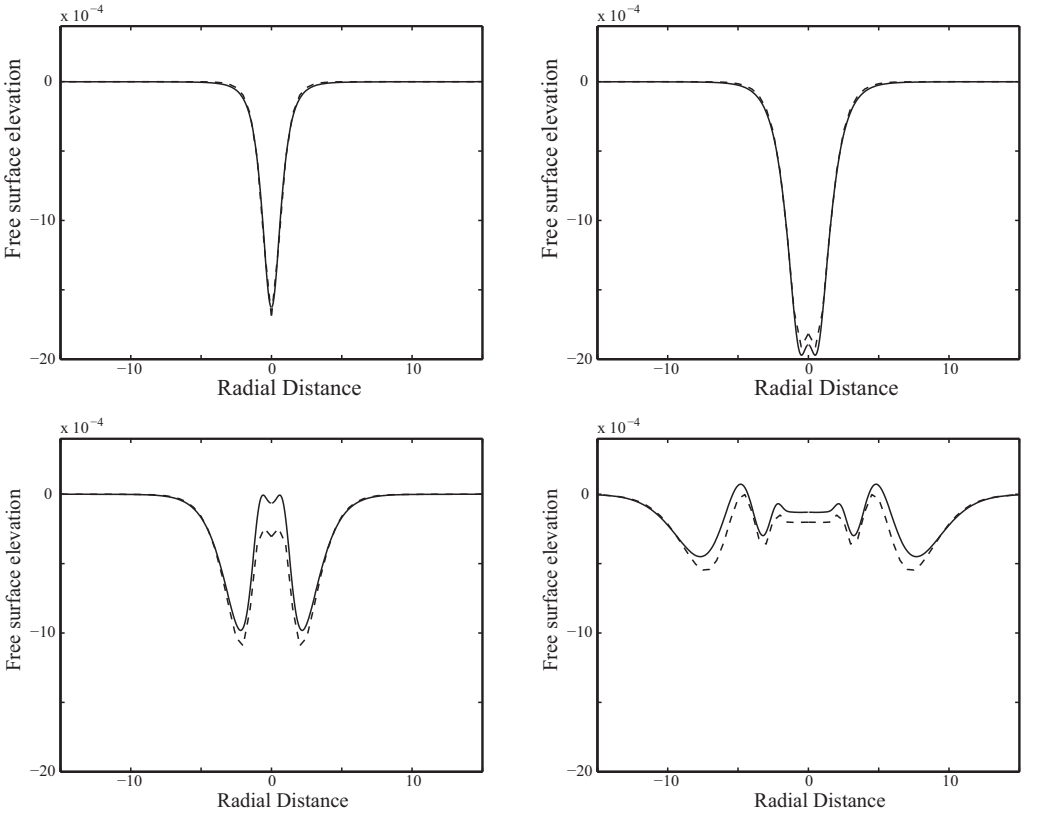

FIGURE 1. Free surface profile for $F = 10^{-3}$ and $H = 1$ (linearised solution dashed) at times $t = 0.5, 2, 4, 10$.

As in earlier work, an impulsively started sink flow leads to an instantaneous downward motion of the surface. If the Froude number is large enough, the free surface draws down directly into the sink. This is illustrated in Figure 2 for a large Froude number of $F = 1$, in the case of a sink positioned at mid-depth in the reservoir (so total depth $H = 2$). If the Froude number is very small, the initial dip soon reverses, and the central point returns to stagnation level, with a steady flow gradually evolving as described earlier: see Figure 3.

In the case of a source flow, there is an upwards bulge initially (with instantaneous upwards velocity). If the flow strength is great enough, the simulations will break down after a fairly short period; if sufficiently small, convergence to a steady state occurs as for sink flows.

Note that in the two-dimensional (line sink) finite depth case, there was a change in local fluid depth upon initiation of the flow, with a wave emanating from above the line sink travelling at constant velocity out to infinity and reducing (increasing in the case of a source flow) the local reservoir depth. Predicted by shallow water theory and observed in both [19] and [28] for planar flow, this change in depth is neither predicted nor observed in the current axisymmetric case. However, there is a disturbance to the free surface that

https://doi.org/10.1017/S0956792516000310 Published online by Cambridge University Press

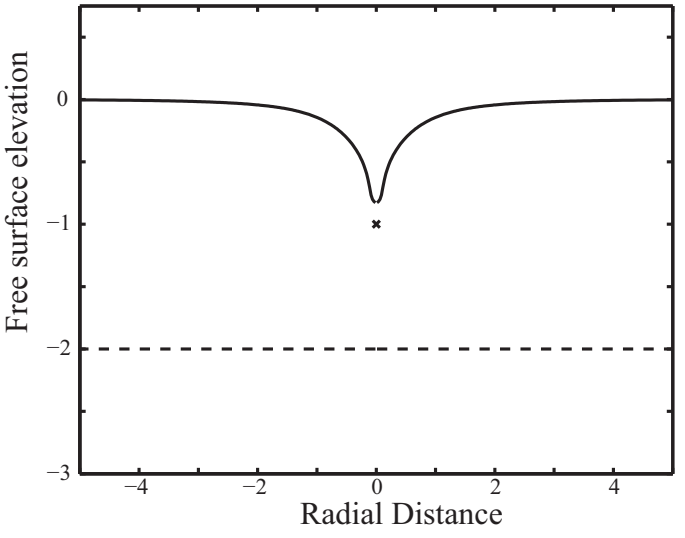

FIGURE 2. An imminent drawdown: $H = 2, F = 1$, at time $t = 0.19$. The dashed line is the reservoir base.

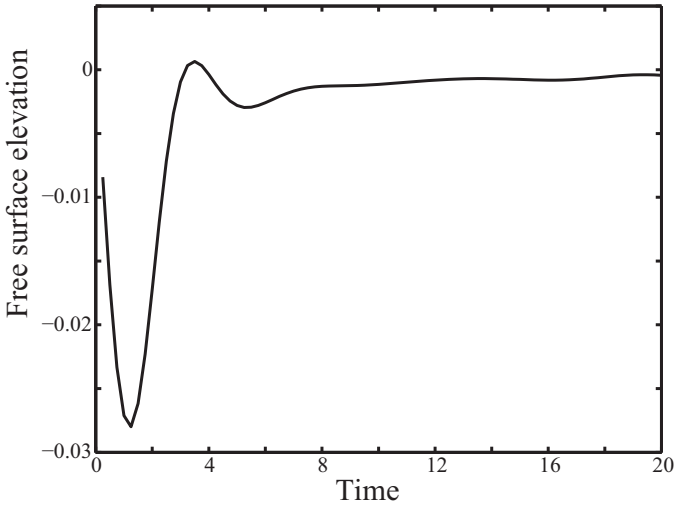

FIGURE 3. Depth of central point over time: $H = 1, F = 0.01$.

decreases in amplitude as it travels out to infinity. This disturbance is larger for smaller values of total depth H.

There is relatively little difficulty in identifying the critical drawdown Froude number for the case of an impulsive flow, and a plot of this against sink depth appears as the dashed curve in Figure 4. It can be seen that there is a steady increase in critical Froude number (representing the sink strength) as the depth of the fluid is increased. Note in particular that the "mid-way" sink placement ($H = 2$) gives a critical value far closer to the infinite depth case than to the bottom flux case.

https://doi.org/10.1017/S0956792516000310 Published online by Cambridge University Press

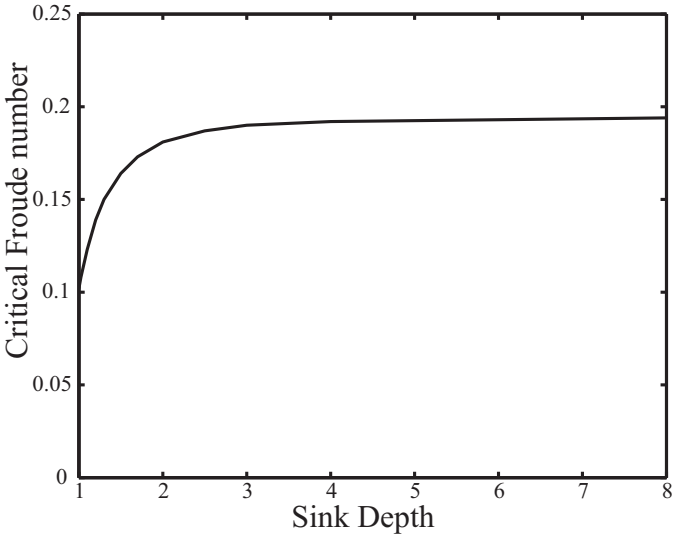

FIGURE 4. Smallest Froude number for which drawdown from an impulsive start is guaranteed.

The results agree well with those given in Xue and Yue [33] for large total depth H: they obtained a value of 0.1931 for the onset of drawdown, whereas we observe a higher value of 0.197. (Note that the accuracy was much higher in our case, with a spatial separation of $\delta r = 0.05$ used in [33], although a boundary integral method was used there.)

Xue and Yue in [33] observed a "transcritical" regime in which the fluid spikes upwards as drawdown looks imminent, for values just below the critical drawdown value, and we see some evidence of this for $F = 0.196$. For smaller values still, it was claimed in [33] that the flow was seen to transition to a steady flow. They examined the case $F = 0.1$ in some detail. However, our simulations indicate that this situation is not typical for all F below the "transcritical" regime. Instead, for all values of total depth H, it was evident that for a reasonably large range of subcritical flows, breaking waves associated with the central swell lead to the simulations breaking down, so it is impossible to determine whether evolution to a steady state would follow. Indeed, in our case, the simulations broke down soon after the lowest point was achieved, unless F was reduced well below the critical drawdown value.

In Figure 5, we give the free surface profile at four moments for the infinite depth case (strictly, $H = 1000$), for the subcritical value $F = 0.18$. The first figure is just prior to the lowest point of descent of the central point and the second soon after the reversal has begun. For lower Froude numbers, the ascent would continue smoothly up to the stagnation height, but in this case already the third figure suggests this will not happen, and indeed in the final figure, it can be seen that small breaking waves are forming, the simulation breaking down very soon after. This seems to happen over a fairly wide range of subcritical Froude numbers (either sooner or later). However, we were able to replicate the results in [33] for the value $F = 0.1$, where a smooth transition to a stagnation point steady flow was observed.

https://doi.org/10.1017/S0956792516000310 Published online by Cambridge University Press

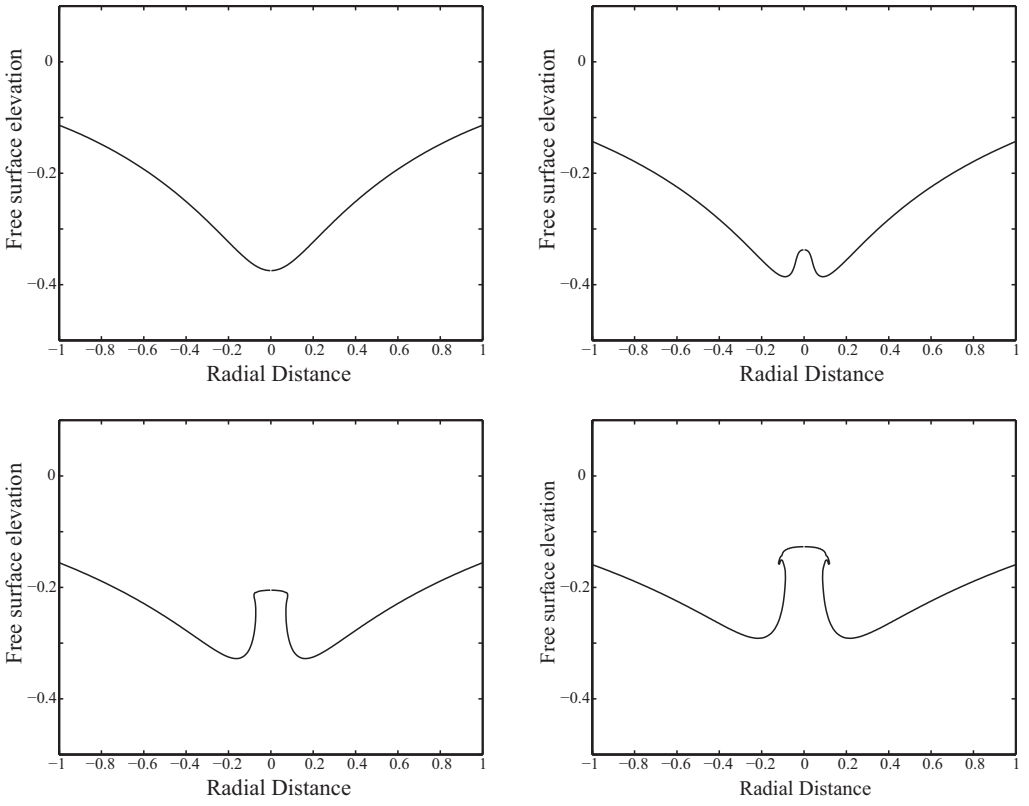

FIGURE 5. Free surface profile in impulsive case with $H = 1000$ and $F = 0.18$ at times $t = 1.00, 1.40, 1.70, 1.87$.

We return to the question of how large F can be for steady states to evolve spontaneously given a suitable flow history.

5.3 Linearly increased sink strength

Of particular relevance to the situation in actual reservoirs is the case in which the Froude number varies smoothly, perhaps asymptotically approaching some final value, or else continuing to increase or decrease for a long period. Perhaps, the simplest case of this is a linear ramp-up of the flow rate, such as a Froude number that is zero at $t = 0$ (at which moment the fluid is quiescent) and which increases according to

$$F(t) = F_0\, t,\ t \geqslant 0.$$

Here, F_0 is the value of $F(t)$ at $t = 1$.

The numerical results we obtained in this case are qualitatively very similar to those previously obtained for a point sink in an infinitely deep fluid. A dip (or bulge in the source flow case) will develop that takes a form given by the first term in equation (3.8) and maintains itself over a moderately long period, matching the linearised solution until non-linear effects become evident. This pseudo-steady state arises regardless of the depth

https://doi.org/10.1017/S0956792516000310 Published online by Cambridge University Press

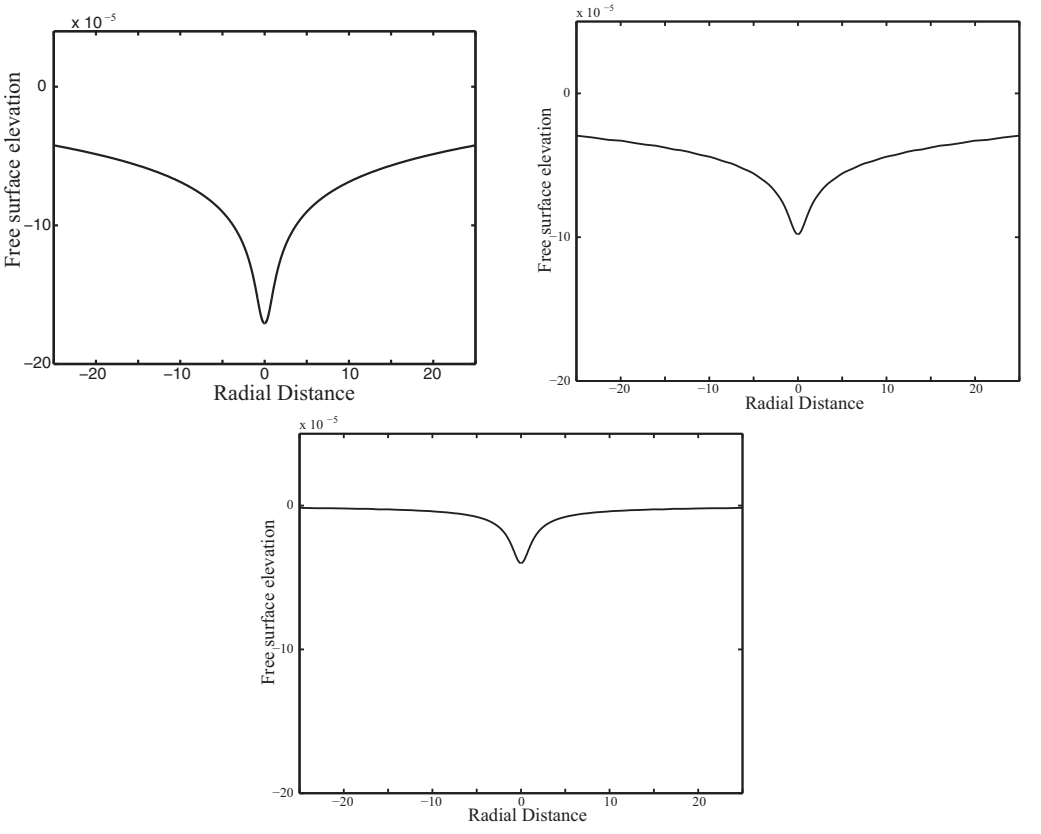

FIGURE 6. Free surface profile for moderately large time if $F(t) = (2 \times 10^{-5})t$: (a) $H = 1$, (b) $H = 2$, (c) $H = \infty$.

of the sink (its size depending linearly on F_0). This dip (bulge) term shows up readily in the simulations. In Figure 6, the dip can be seen for total depth $H = 1, 2, \infty$ in the case of a sink flow for which $F_0 = 2 \times 10^{-5}$: the dip spreads out quite far along the horizontal domain for $H = 1$ and is generally deeper, but narrows considerably and is not as deep at $r = 0$ as the bottom moves downward from the sink.

Of course, as the Froude number continues to ramp up without bound, non-linear effects start to dominate, and eventually the simulation will break down. Typically, an approximation of a stagnation point steady state flow (which depends on F^2) superimposes itself on the dip term, and ultimately the simulations break down because cusps form on the surface at the two secondary dips. If the ramping up is sufficiently rapid, a drawdown similar to the impulsive case may be observed in a sink flow.

In fact, as discussed in Section 3.2, the dip term appears to influence the behaviour of the free surface for flows in which the Froude number varies non-linearly as well: The free surface tends to be displaced from the horizontal in accord with the dip term by an amount proportional to the derivative $F'(t)$ (which is of course constant in the case of a constant ramp-up/down).

https://doi.org/10.1017/S0956792516000310 Published online by Cambridge University Press

Also of interest is the possibility of drawdown arising from the linearly increased flow. For large enough values of F_0 in $F = F_0 t$, the free surface draws down directly into the sink, just as with sufficiently strong constant flows. However, for small enough F_0, this initial drawdown is averted and the dip term discussed above asserts itself for a period, presumably prior to some form of subsequent drawdown, possibly at the sides of the dip rather than the central point. However, in between these cases, the situation proved to be quite unclear, and no meaningful critical values could be obtained: There was no obvious threshold for any value of total depth H that could be considered a critical value.

5.4 Impulsive flows that rapidly decay to zero

Sometimes fluid can be extracted from a reservoir in a short sharp burst. There is interest in whether the burst is sufficiently intense to induce a drawdown, even though it may be very short-lived. We considered the case in which the flow is initiated impulsively at time $t = 0$ according to $F(t) = F_0(k \exp(-kt))$, where k is assumed large. Such a flow has initial value $F_0 k$ but rapidly dies away to zero. The reason for this form for $F(t)$ is that the total flux drawn from the reservoir is then F_0, most of it extracted a very short time after $t = 0$.

In this situation, a very much smaller time increment was used in the numerics ($\delta t = 1/(1000k)$ proved sufficient), since the time to drawdown was generally very short (typically $t \approx 0.015$, compared to $t > 1$ in the impulsive case). The fluid would typically dip far closer to the sink without drawdown being inevitable in this case. The central point drops very rapidly towards the sink, and then either rebounds as $F(t)$ drops rapidly towards zero, or appears to drawdown into the sink before this can happen (although there is a transitional phase in which the surface seems to spike, just below the critical drawdown value, just as with the constant strength impulsive flow case). If drawdown is clearly averted, the central point seems to rise up at a linear rate, through the stagnation level and continuing upwards, to form a high spike, at which point the simulations fail. (For small F_0, this spike is not apparent, the free surface simply returning to the stagnation level.)

Obtaining accurate drawdown values was rather delicate. In Figure 7, we show the behaviour of the surface at $r = 0$ with total depth $H = 4$, for the subcritical value $F = 0.259$ just prior to the simulation breaking down, and next to it the same for the critical value of $F = 0.260$, where the slight turn-back and subsequent upwards spike is absent. It is possible that the upward spike, which occurs over a single time increment only, is some form of numerical instability, although the levelling off prior to it seems real. Similar behaviour is observed in [33] in the case of an impulsive (constant strength) flow, where a very small window of subcritical cases in which the surface spikes is noted (their so-called transcritical cases).

We found that the critical value for F_0 to guarantee drawdown depended very little on the precise value of k providing $k > 10$ (only the time-scale of the problem varying with k), suggesting that this is a meaningful critical value. Moreover, very similar results were obtained by letting $F(t)$ be a step function with some large finite value for a very short time (so that the total flux withdrawn is one unit multiplied by some factor F_0), followed by a small positive value thereafter (necessarily non-zero since otherwise there is no sink for the surface to draw into!).

https://doi.org/10.1017/S0956792516000310 Published online by Cambridge University Press

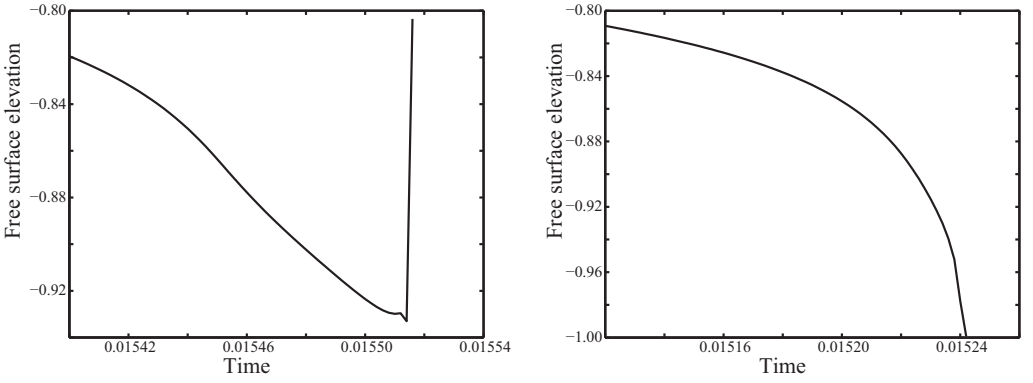

FIGURE 7. Behaviour of central point for slightly different values of F_0 in $F(t) = F_0(k\exp(-kt))$, with $H = 2.5$: on the left $F_0 = 0.259$, and on the right $F_0 = 0.260$.

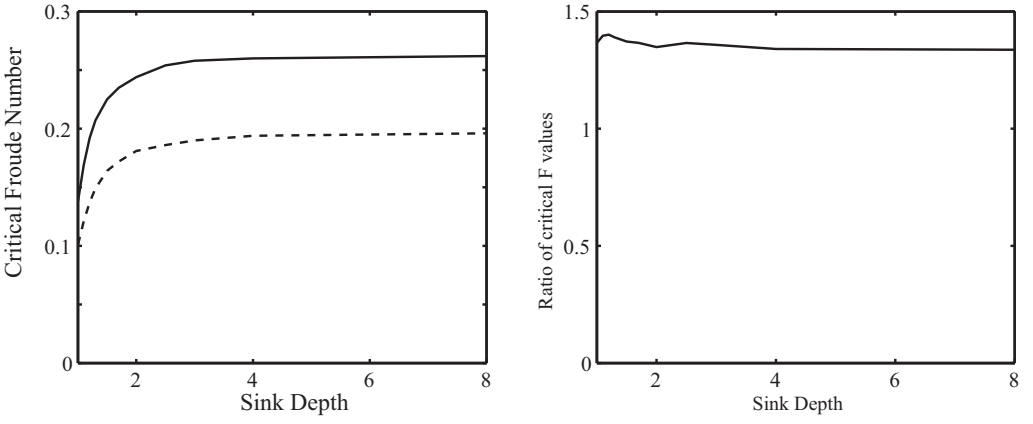

FIGURE 8. (a) Smallest F_0 such that $F(t) = F_0(k\exp(-kt))$ draws down (impulsive case dashed), (b) ratio of current critical value to impulsive, against total depth H.

In Figure 8(a), a plot of the critical F_0 against total depth H is given, with the constant impulsive critical flow rates shown dashed. It is not to be expected that the two sets of data would be of roughly the same size, but it can be seen that the variation with submergence depth is quite similar in both cases. Indeed, in Figure 8(b), the ratio of these two critical values is given; evidently, the ratio between the two is almost constant.

5.5 Obtaining history-independent critical flow rates

As in earlier work ([26–28]), there is considerable interest in answering the following two related questions: of those flows which smoothly ramp up to some final value, what is the smallest ultimate Froude number to guarantee drawdown, and what is the largest ultimate Froude number at which steady flows can evolve?

For this purpose, we considered flow histories for which the rate asymptotically approached some final value, using an exponential shape function. We increased this limiting

https://doi.org/10.1017/S0956792516000310 Published online by Cambridge University Press

value in successive simulations. Again, the ramp-up function had the form

$$F(t) = F_0(1 - \exp(-t/K)),\ t \geqslant 0,$$

this time for some large positive constant K (typically $K = 10$ was sufficiently large in the simulations). For small time, $F(t) \approx F_0 t/K$, whilst for large time, $F(t) \to F_0$.

For small F_0, the initial sink flow generated a dip (or swell, in the case of a source flow) as discussed previously, with magnitude proportional to the rate of change of F and which would therefore slowly reduce in size. This was backed up by the linearised solution. In the simulations, this dip was overlaid by a stagnation point steady flow that increasingly dominated (being proportional to F^2).

Previous work on steady states in both the finite and infinite depth cases of the axisymmetric problem considered here appeared to establish the existence of limiting stagnation point steady flows in which a secondary stagnation ring is present; in the terms used here, this occurs for $F \approx 0.5$ in the infinite depth case (see [2]), and for $F \approx 0.26$ in the bottom flux case $H = 1$ (see [13]). However, recent more accurate work presented in [14] seems to show that the solutions with a stagnation ring are not actually steady solutions, but an artefact of inaccuracies in the numerical scheme and limitations of the computational power available at that time. This result is consistent with the work of [6] where no such solutions were found. As reported in [27], no such steady states were observed in the case of a point sink flow in a fluid of infinite depth. We were not able to observe them in the current work either, even for source flows.

For both source and sink flows, it was found that there was a maximal value of F above which steady solutions did not seem to evolve (instead, the simulations would rather abruptly break as the critical value was surpassed). For a given sink depth, there was a small difference between the critical values for sources and sinks, which seemed to be due to the fact that for sources there was an inital upward movement of the surface and for sink flows, an initial downward movement, and as time progressed, the surface would slowly return to stagnation level. For near-critical Froude number values, this would mean a slightly earlier breakdown in sink flows because the sink submergence depth was effectively slightly lower than for source flows. For source flows converging to the claimed critical value, the free surface always returned to the stagnation level well prior to a breakdown, suggesting these values are quite reliable.

Thus, it became evident that for each value of total depth H, there was a maximal Froude number at which steady flows could evolve. For example, in the infinite depth case, this maximal Froude number was approximately $F = 0.236$, and for the bottom flux case ($H = 1$), it was $F = 0.098$; these values compare quite well to the maximal F for which steady states could be obtained, as found in [14] and [6] of $F = 0.24$ and $F = 0.12$, respectively. For simulations that were ramped up to a final value slightly above the critical Froude number, the surface would either begin to "jiggle" in a seemingly rapidly oscillatory way (for smaller H), or else instabilities would form on the side of the central swell leading to breakdown of the simulations (larger H).

Significantly, there were no secondary waves present in any converged steady solutions we obtained (although these were present to varying degrees when less accuracy was used). A plot of the evolved steady flow near the critical flow rate is given in Figure 9 for

https://doi.org/10.1017/S0956792516000310 Published online by Cambridge University Press

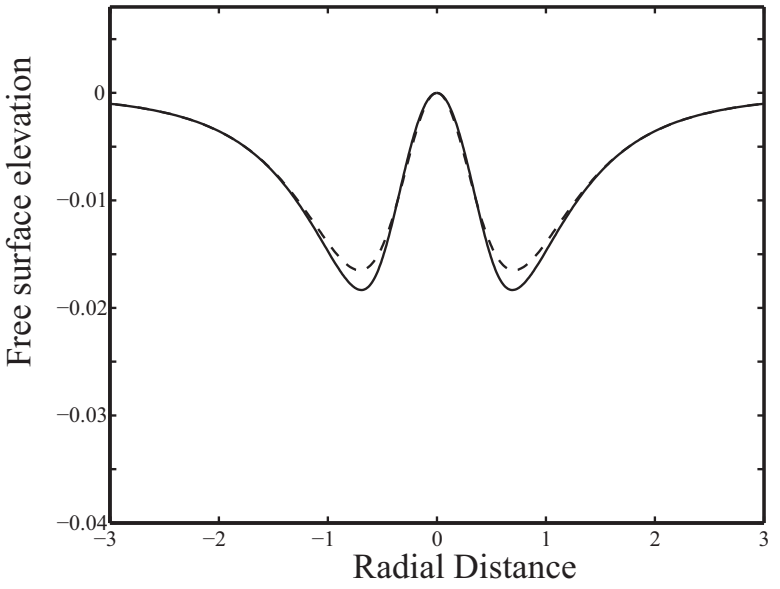

FIGURE 9. An evolved steady state in the infinite depth case, as F is ramped up in a source flow to $F = 0.236$, $t = 100$. The dashed line is the asymptotic steady state.

the infinite depth case, with the asymptotic stagnation point steady solution of the form $-F^2 y_2(r)$ as in equation (3.8) in Section 3.2 dashed.

Similar behaviour was observed for each finite choice of total depth H considered. The critical values for the existence of steady states increased as the reservoir depth increased from $H = 1$, though then only minimally after $H = 2$. A plot of critical Froude number against H is given in Figure 10(a), which shows the largest F at which steady flows can evolve from an unsteady source flow. In Figure 10(b), the ratio of the current critical value to the impulsive one is plotted against H. It can be seen that the two critical values are almost identical in the bottom flux case, with the steady critical value actually lower than the impulsive one, but this quickly reverses, and a more or less constant ratio establishes as H increases above 3.

5.6 Drawdowns for flows ramping to a final value

In practice, a flow often increases smoothly from zero up to some final value. To model this, we used a shape function of the same general form as in the previous section: $F(t) = F_0(1 - \exp(-t/K))$, $t \geqslant 0$, where K is some positive value.

For K close to zero, this flow is close to an impulsively initiated constant strength flow, covered above, so there is no point considering this case again. On the other hand, if K is very large, then the situation modelled is basically the one considered in the previous section – a slow ramping up, initially effectively linear ($F(t) \approx F_0 t/K$ for $t \ll K$), and levelling off to some final value – albeit over a different range of F-values. It is likely that for such flow shapes, any observable drawdown will be in the approximately linear phase,

https://doi.org/10.1017/S0956792516000310 Published online by Cambridge University Press

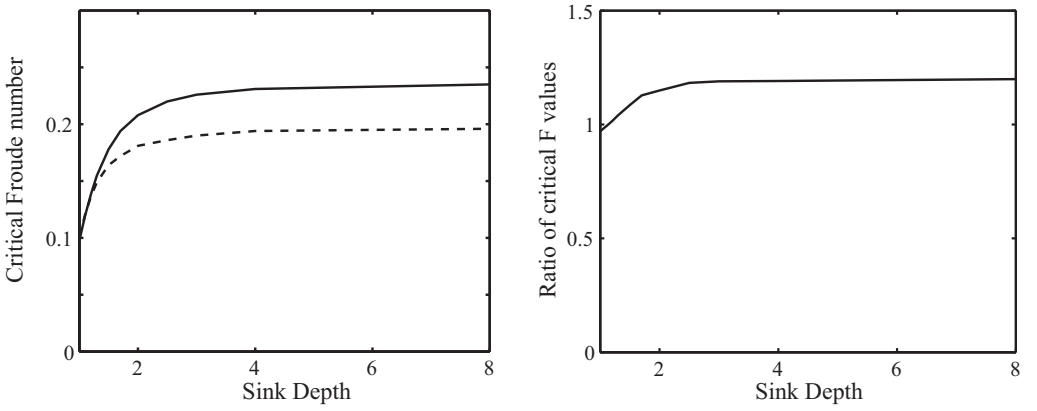

FIGURE 10. (a) Largest Froude number for which steady flows can evolve (and drawdown be can averted in a sink flow) against H. (Impulsive critical drawdown values are shown in the dashed curve.), (b) ratio of the critical values plotted in (a).

and we are back to another case considered earlier, in which no convincing critical values could be obtained.

So we (somewhat arbitrarily) chose $K = 1$, and so a shape function of $F(t) = F_0(1 - \exp(-t))$, $t \geqslant 0$. This proved to give rather clear drawdown critical values, with drawdown always coming at a stage in which the asymptotic (large time) value of $F(t)$ was not far off. For cases in which drawdown was only narrowly averted, the simulations often broke down soon after that point, perhaps due to small breaking waves. It is possible that in an actual physical flow, a delayed drawdown may subsequently occur as F was increased towards its final value. So these critical values must be treated with some caution, but they do indicate that there is more than one possible notion of "critical flow rate", even if one is interested only in drawdown.

In Figure 11(a), the smallest value that guarantees drawdown using this shape function is given, with the impulsive and steady critical values the two dashed curves, for comparison. In Figure 11(b), the ratio of the current critical value to the impulsive one is given: it can be seen that the ratio is close to constant across the range of H-values.

Thus, for the bottom flux case $H = 1$, the critical value of $F = 0.127$ was not surprisingly considerably higher than the critical flow rate guaranteeing drawdown in an impulsive flow ($F = 0.101$), hence also higher than the largest F-value guaranteeing the existence of steady flows below it ($F = 0.098$, since $0.101 > 0.098$!). But even the $H = 2$ mid-depth case, in which steady flows can exist well above the impuslive critical drawdown value, this number went up to $F = 0.226$ (compared to 0.181 and 0.208, respectively). So in both cases, there is a significant region of F-values in which drawdown will be averted yet steady flows cannot evolve. This is not the case for impulsive flows. The same phenomenon was repeated across the range of possible submergence depths.

6 Conclusions

In this work, we set out to discover if the inclusion of a rigid base in a reservoir made a significant difference to the flow patterns generated by a point source or sink. The

https://doi.org/10.1017/S0956792516000310 Published online by Cambridge University Press

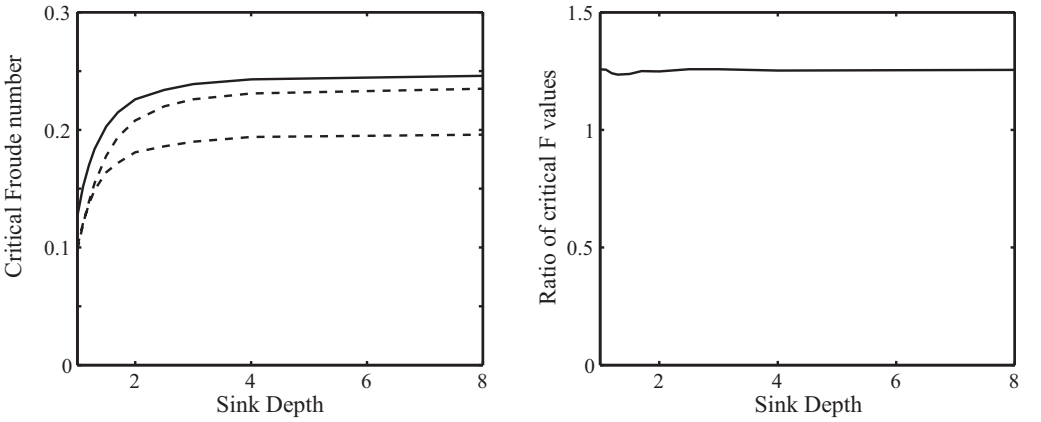

FIGURE 11. (a) Critical drawdown values F_0 for $F(t) = F_0(1 - e^{-t})$ against H. (Impulsive critical drawdown and critical steady values dashed.), (b) ratio of current critical value to impulsive, against H.

evidence is clear that although there are some differences, they are more quantitative than qualitative. The general behaviour is much the same, even quantitatively if the source/sink is located at least half-way up the fluid.

Thus, as in previously considered cases of withdrawal problems, there are at least two effective critical values of Froude number depending on the flow history. Drawdown from an impulsive start depends largely on the initial dip formed in the surface, giving rise to one critical value of F. We showed that this critical value increases with reservoir depth, but does not increase much once the sink is at least half-way down the reservoir. It seemed that for a wide range of subcritical flows, breaking waves would be generated soon after the point at which the free surface avoided drawdown, with a smooth transition to a steady flow only occurring for sufficiently small Froude number. The same things are observed when a sudden impulsive flow is initiated which rapidly decays towards zero, or when a moderately rapidly increasing flow approaches a final value.

If initial drawdown is avoided because the flow rate is increased gradually, then the flow will progress for some time (up to a higher Froude number), possibly achieving a steady state at some final Froude number value. For both source and sink flows, we were able to find the largest Froude number at which steady flows could evolve and maintain themselves. This critical value increased rapidly as the sink was moved off the reservoir base, and was considerably higher than the impulsive drawdown value except near the bottom flux case of $H = 1$.

No observed steady flows showed any signs of waves. Also, we were unable to observe evolution to steady flows featuring secondary stagnation rings (or their pre-cursors) as described in [2] and [13]. This, and the results of simulations in this range of Froude numbers, suggest strongly that either such steady flows are unstable, or else are spurious due to insufficient accuracy. Maximal steady state solutions obtained in the current work are consistent with those of [14] and [6].

By ramping up to a final value of F with moderate speed, it was shown that drawdown could be averted for F-values well above the range over which steady flows exist, across

https://doi.org/10.1017/S0956792516000310 Published online by Cambridge University Press

the range of sink submergence depths. This suggests that flows that are neither steady nor involve any form of drawdown can exist, and may in practice involve breaking waves.

References

[1] Craya, A. (1949) Theoretical research on the flow of nonhomogeneous fluids. *La Houille Blanche* **4**(2), 44–55.

[2] Forbes, L. K. & Hocking, G. C. (1990) Flow caused by a point sink in a fluid having a free surface. *J. Austral. Math. Soc.* Ser. B **32**(2), 233–252.

[3] Forbes, L. K. & Hocking, G. C. (1993) Flow induced by a line sink in a quiescent fluid with surface-tension effects. *J. Austral. Math. Soc.* Ser. B **34**(3), 377–391.

[4] Forbes, L. K. & Hocking, G. C. (1995) The bath-plug vortex. *J. Fluid Mech.* **284**, 43–62.

[5] Forbes, L. K. & Hocking, G. C. (2003) On the computation of steady axi-symmetric withdrawal from a two-layer fluid. *Comput. Fluids* **32**(3), 385–401.

[6] Forbes, L. K., Hocking, G. C. & Chandler, G. A. (1996) A note on withdrawal through a point sink in fluid of finite depth. *J. Austral. Math. Soc.* Ser. B **37**(3), 406–416.

[7] Gariel, P. (1949) Experimental research on the flow of nonhomogeneous fluids. *La Houille Blanche* **4**, 56–65.

[8] Hocking, G. C. (1985) Cusp-like free-surface flows due to a submerged source or sink in the presence of a flat or sloping bottom. *J. Aust. Math Soc.* Ser. B **26**(APR), 470–486.

[9] Hocking, G. C. (1991) Withdrawal from two-layer fluid through line sink. *J. Hydr. Engng* ASCE **117**(6), 800–805.

[10] Hocking, G. C. (1995) Supercritical withdrawal from a two-layer fluid through a line sink. *J. Fluid Mech.* **297**, 37–47.

[11] Hocking, G. C. & Forbes, L. K. (1991) A note on the flow induced by a line sink beneath a free surface. *J. Aust. Math Soc.* Ser. B **32**(3), 251–260.

[12] Hocking, G. C. & Forbes, L. K. (2001) Supercritical withdrawal from a two-layer fluid through a line sink if the lower layer is of finite depth. *J. Fluid Mech.* **428**, 333–348.

[13] Hocking, G. C., Vanden Broeck, J.-M. & Forbes, L. K. (2002) A note on withdrawal from a fluid of finite depth through a point sink. *ANZIAM J.* **44**(2), 181–191.

[14] Hocking, G. C., Forbes, L. K. & Stokes, T. E. (2014) A note on steady flow into a submerged point sink. *ANZIAM J.* **56**(2), 150–159.

[15] Hocking, G. C., Stokes, T. E. & Forbes, L. K. (2010) A rational approximation to the evolution of a free surface during fluid withdrawal through a point sink. *ANZIAM J.* Ser. E **51**, E31–E36.

[16] Huber, D. G. (1960) Irrotational motion of two fluid strata towards a line sink. *J. Engng. Mech. Div.* Proc. ASCE, 86, EM4, 71–85.

[17] Imberger, J. & Hamblin, P. F. (1982) Dynamics of lakes, reservoirs and cooling ponds. *Ann. Rev. Fluid Mech.* **14**, 153–187.

[18] Jirka, G. H. & Katavola, D. S. (1979) Supercritical withdrawal from two-layered fluid systems, part 2 three-dimensional flow into a round intake. *J. Hyd. Res.* **17**(1), 53–62.

[19] Landrini, M. & Tyvand, P. A. (2001) Generation of water waves and bores by impulsive bottom flux. *J. Engng. Maths* **39**(1–4), 131–171.

[20] Lawrence, G. A. & Imberger, J. (1979) *Selective Withdrawal Through a Point Sink in a Continuously Stratified Fluid with a Pycnocline. Tech. Report No. ED-79-002*, Dept. of Civil Eng., University of Western Australia, Australia.

[21] Lubin, B. T. & Springer, G. S. (1967) The formation of a dip on the surface of a liquid draining from a tank. *J. Fluid Mech.* **29**, 385–390.

[22] Lustri, C. J, McCue, S. W. & Chapman, S. J. (2013) Exponential asymptotics of free surface flow due to a line source. *IMA J. Appl. Math.* **78**(4), 697–713.

[23] Miloh, T. & Tyvand, P. A. (1993) Nonlinear transient free-surface flow and dip formation due to a point sink. *Phys. Fluids A* **5**(6), 1368–1375.
[24] Sautreaux, C. (1901) Mouvement d'un liquide parfait soumis à lapesanteur. Dé termination des lignes de courant. *J. Math. Pures Appl.* **7**, 125–159.
[25] Scullen, D. & Tuck, E. O. (1995) Non-linear free-surface flow computations for submerged cylinders. *J. Ship Res.* **39**(3), 185–193.
[26] Stokes, T. E., Hocking, G. C. & Forbes, L. K. (2002) Unsteady free surface flow induced by a line sink. *J. Eng. Math.* **47**(2), 137–160.
[27] Stokes, T. E., Hocking, G. C. & Forbes, L. K. (2005) Unsteady flow induced by a withdrawal point beneath a free surface. *ANZIAM J.* **47**(2), 185–202.
[28] Stokes, T. E., Hocking, G. C. & Forbes, L. K. (2008) Unsteady flow induced by withdrawal in a fluid of finite depth. *Comput. Fluids* **37**(3), 236–249.
[29] Tuck, E. O. (1997) Solution of nonlinear free-surface problems by boundary and desingularised integral equation techniques. In: J. Noye *et al.* (editors), *Proc. 8th Biennial Computational Techniques and Applications Conference,* World Scientific, Singapore, pp. 11–26.
[30] Tuck, E. O. & Vanden Broeck, J.-M. (1984) A cusp-like free-surface flow due to a submerged source or sink. *J. Aust. Math Soc. Ser. B* **25**(APR), 443–450.
[31] Vanden Broeck, J.-M. & Keller, J. B. (1987) Free surface flow due to a sink. *J. Fluid Mech.* **175**, 109–117.
[32] Wehausen, J. V. & Laitone, E. V. (1960) Surface waves. In: *Encyclopaedia of Physics*, Vol. IX, Springer-Verlag, Berlin, pp. 446–778.
[33] Xue, M. & Yue, D. K. P. (1998) Nonlinear free-surface flow due to an impulsively started submerged point sink. *J. Fluid Mech.* **364**, 325–347.
[34] Yih, C. S. (1980) *Stratified Flows*, Academic Press, New York, pp. 110–121.